Table 1. Baseline Characteristics

n=967 (1199*)	Control* (n=277) (509*)	DCM (n=383)	HCM (n=307)	P NA
Demographics				
Male/female	129 (46)/148 (54)	214 (56)/169 (44)	167 (54)/140 (46)	0.046
Caucasian/African American	193 (70)/84 (30)	204 (53)/179 (47)	258 (84)/49 (16)	<0.001
Age, y	44.24±17.50	51.43±13.92	52.40±16.23	<0.0001
BMI, kg/m^2	28.04±7.22	30.15±7.48	30.19±7.21	0.0003
BSA, m^2	1.96±0.32	2.07±0.33	2.05±0.29	<0.0001
DM, %	26 (10)	90 (23)	35 (12)	<0.001
Smoker, %	26 (10)	57 (15)	49 (17)	<0.001
Heart rate, bpm	71.3±12.4	80.1±16.2	70.4±12.0	<0.0001
Systolic BP, mm Hg	123.5±15.7	116.8±16.8	128.5±17.5	<0.0001
Diastolic BP, mm Hg	73.3±9.9	73.4±12.4	74.3±13.4	0.5315
Echocardiographic data				
ST, cm	0.96±0.18	1.01±0.22	1.89±0.48	<0.0001
PWT, cm	0.97±0.2	1.08±0.23	1.34±0.32	<0.0001
LVEDD, cm	4.51±0.53	6.28±0.97	4.15±0.67	<0.0001
LVESD, cm	2.90±0.53	5.39±1.12	2.45±0.70	<0.0001
LVM, g	184.26±65.97	350.83±142.24	355.89±128.24	<0.0001
LVMI, g/m^2	94.02±25.12	169.50±63.22	173.30±63.22	<0.0001
LA size, cm	3.46±0.76	4,43±1.00	4.25±0.79	<0.0001
LVEF	61.47±5.37	24.42±8.04	67.03±5.15	<0.0001

HCM indicates hypertrophic cardiomyopathy; DCM, dilated cardiomyopathy; NA, not applicable; BMI, body mass index; BSA, body surface area; DM, diabetes mellitus; BP, blood pressure; ST, septal thickness; PWT, posterior wall thickness; LVEDD, left ventricular end-diastolic diameter; LVESD, left ventricular systolic diameter; LV mass, left ventricular mass; LVMI, left ventricular mass indexed to body surface area; LVEF, left ventricular ejection fraction; and LA, left atrium.

*Denotes the total number of the control group with data that are included in the table. We added a second control group of African American individuals (n=232) who had normal ECGs and echocardiograms but did not have the detailed data.

based G-LISA RhoA activation assay biochemistry kit (Cytoskeleton, Denver, CO), as described.[8] We isolated total protein 2 days after transduction of NRCM with the recombinant adenoviruses per instruction of the manufacturer. We equalized the total protein concentrations among the samples at 1 mg/mL for the assay and measured the signals at an absorbance of 490 nm, using a microplate spectrometer.

RNA Extraction and Quantitative Reverse Transcriptase–PCR

We isolated total cellular RNA from NRCM using an RNeasy Mini Kit (QIAGEN, Inc). We performed quantitative reverse transcriptase–PCR (qPCR) to quantify mRNA expression levels of rat ANP (Nppa), B-type natriuretic peptide (BNP or Nppb), and rat skeletal α-actin (SkA or Acta1) in NRCM transduced with WT or mutant MURC constructs, as described.[8] Sequences of oligonucleotide primers are shown in online-only Data Supplement Table I.

Cardiac Myocyte Size

Cardiac myocytes were infected with the recombinant adenoviruses and cultured under serum-free conditions for 48 hours. Cells were then fixed with 4% paraformaldehyde and stained with fluorescein isothiocyanate–conjugated phalloidin (SIGMA) for the detection of actin filaments. DNA was stained with 4′,6-diamidino-2-phenylindole. We measured myocyte surface area using Image software (National Institutes of Health, Bethesda, MD) in at least 100 cells per group.

Statistics

Statistical analyses were similar to those published recently.[7,16] We expressed the continuous variables that followed normality distribution as mean±SD. We compared differences among the continuous variables that satisfied the normality distribution by 1-way ANOVA and applied the Bonferroni correction to multiple-comparison tests. Variables that were not normally distributed were compared by Kruskal-Wallis test. We analyzed differences in the categorical variables by χ^2 test.

All in vitro experiments were performed at least 3 times, and the mean values of the 3 measurements were used. Data are expressed as mean±standard error and analyzed by 1-way ANOVA with Scheffe post hoc analysis. A value of $P<0.05$ was considered significant. All statistical analyses were performed using STATA v 10.1.

Results

Characteristics of the Study Population

Phenotypic characteristics of the study population are shown in Table 1 and are partly published.[7,12]

MURC Sequence Variants

We found 6 DCM-specific heterozygous missense variants (p.N128K, p.R140W, p.L153P, p.S307T, p.P324L, and p.S364L) in 8 probands (Table 2). These variants were absent in 509 normal individuals. The p.N128K variant cosegregated with DCM in 2 affected family members and was absent in 5 unaffected family members (Figure 1). The p.S307T was present in 4 adult family members, of whom 3 had severe DCM (Figure 1). One young adult (31 years old) and 1 child also had the p.S307T variant, whereas 3 phenotypically

Table 2. Nonsynonymous Variants Detected in Probands With Dilated Cardiomyopathy

		Control Subjects (n=509)		DCM (n=383)		HCM (n=307)	
Amino Acid	Nucleotide	A 316	C 193	A 179	C 204	A 49	C 258
p.N128K	g.474C>G	0	0	1	0	0	0
p.R140W	g.7721C>T	0	0	0	1	0	0
p.L153P	g.7761T>C	0	0	1	0	0	0
p.S307T	g.8223G>C	0	0	0	1	0	0
p.P324L	g.8274C>T	0	0	3	0	0	0
p.S364L	g.8394C>T	0	0	1	0	0	0
Total No. of nonsynonymous variants per group and ethnic background		0	0	6	2	0	0
Total No. of nonsynonymous variants per group		0 (0 %)		8 (2.1%)		0 (0%)	

DCM indicates dilated cardiomyopathy; HCM, hypertrophic cardiomyopathy; A, African American; and C, Caucasian.

normal adults had the WT genotype. Segregation analysis that includes healthy individuals in cardiomyopathies is subject to age-dependent and incomplete penetrance. The absence of a clinical phenotype in young mutation carriers in this family may reflect partial and age-dependent penetrance of the variant. Collectively, the p.N128K and p.S307T variants were present in 5 affected family members and absent in 8 of 9 clinically normal members (χ^2=8.5, P=0.003). The small size of these 2 families and the incomplete penetrance of the p.S307T variant impeded the power to calculate the logarithm of odds score, as a measure of linkage to strengthen the causal role of these variants. The p.P324L was a recurring variant, as it was detected in 3 probands. To determine whether the probands shared a common ancestral allele at the *MURC* locus, we genotyped the 3 families for 3 locus-specific STR markers. The 3 probands did not share the genotypes for the *MURC* locus, indicating independent origins of the mutation in these individuals (online-only Data Supplement Figure I).

We also detected a deletion variant (p.L232-R238del), which excluded 7–amino acid–long motif (ERLRQSG, Swiss-Prot ID: Q5BKX8.2) in 3 probands with HCM, 1 African American, and 2 white subjects. The deletion was absent in >500 control individuals. Two affected members of a HCM family had the deletion variant. However, it was absent in an affected member of another family with the deletion variant (online-only Data Supplement Figure II). The 2 affected family members in the latter family had a p.L907V mutation in MHY7, a known gene for cardiomyopathies.[5] The p.L907V mutation was absent in >500 normal individuals, and affects a highly conserved domain in MYH7 protein. It is predicted to be probably damaging by PolyPhen-2 analysis (score, 0.954; sensitivity, 0.74; specificity, 0.93).

In contrast to 7 phenotype-specific variants, we detected only one nonsynonymous variant (p.R272H) that was present only in the control group (Table 2). The p.R272H was predicted to be a benign variant by PolyPhen-2 analysis. To test whether *MURC* was a disease-causing gene, we performed a gene-centric analysis by coalescing the nonsynonymous variants in each group and comparing the prevalence of *MURC* variants in cases with DCM and control subjects. In support of a causal role of *MURC* variants in DCM, nonsynonymous variants were overrepresented by 25-fold in the cases (Pearson χ^2=7.84, P=0.005).

As would be expected, we identified several polymorphisms that were common to the cases and the control subjects, including 6 nonsynonymous variants, 14 synonymous, and 8 noncoding variants (online-only Data Supplement Tables II and III). The frequencies of the nonsynonymous or synonymous polymorphisms were not significantly different between the cases and control subjects. Likewise, the age distributions of the control individuals and the DCM cases with the nonsynonymous variants were similar. Overall, the minor allele frequencies of the nonsynonymous polymorphisms were <1% in the study population. The most common variant was the p.S78L, which had a minor allele frequency of 0.009 in the entire population and 0.033 in the African American subpopulation. The p.N81K was detected in 3 African Americans, 1 with HCM, 1 with DCM, and 1 normal individual. In each case, it cosegregated with the p.S78L variant.

Mutations in Known Genes for Cardiomyopathies

We sequenced all coding regions and exon-intron boundaries of *MYH7*, *MYBPC3*, *TNNT2*, *TNNI3*, *TPM1*, *ACTC1*, and *LMNA*, known relatively common genes for cardiomyopathies,[4,5] in all *MURC* mutation carriers. An African American patient with DCM had a compound mutation: the p.P324L variant in *MURC* and a novel nonsynonymous variant p.M245T in the *TPM1* gene. Likewise, 1 family member who had the p.L232-R238del variant in *MURC* also had a p.L907V mutation in the *MYH7* gene (probably compound mutation).

We identified 3 nonsynonymous variants in *LMNA* on screening of 103 probands with DCM associated with conduction defect and/or atrial fibrillation.[4] None had a *MURC*

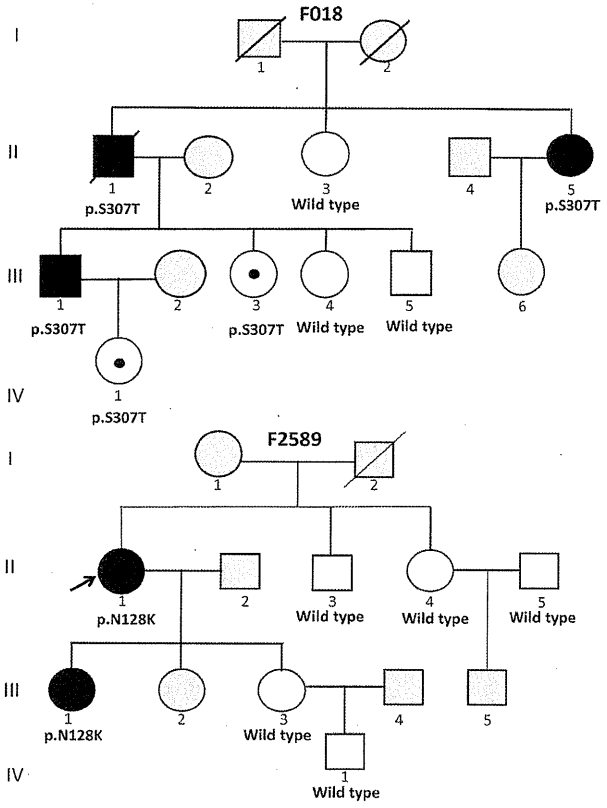

Figure 1. Pedigree of families with Muscle-Restricted Coiled-Coil *(MURC)* mutations: Squares and circles represent male and female members. Full and open circles and squares indicate affected and unaffected (normal) individuals, respectively. Gray squares and circles indicate individuals that were not studied. The mutation and wild-type codons are listed under those members that were studied. Individual III-3, who is 31 years old, is a mutation carrier but is phenotypically normal (nonpenetrance). Individual IV-1 in Pedigree F018 is 5 years old and noncontributory to cosegregation analysis.

mutation. Likewise, we identified 32 different mutations in *MYH7* (14 mutations), *MYBPC3* (11 mutations), *TNNT2* (2 mutations), *TNNI3* (1 mutation), *TPM1* (2 mutations), and *MYOZ2* (2 mutations) in screening of 81 probands with HCM. None had a mutation in *MURC* gene.

Phenotypic Expression of *MURC* Mutation Carriers

The phenotype in the mutation carriers was notable for heart failure in the middle age (mean age, 45.0±6.5 years), leading to severely depressed left ventricular systolic function, which led to cardiac transplantation in 4 affected members. Cardiac tissues were not available to analyze histological correlates of MURC variants. Several affected members exhibited supraventricular arrhythmias and progressive conduction defects, requiring implantation of a permanent pacemaker and internal cardioverter/defibrillator. Detailed phenotypic data are shown in Table 3.

Predicted Pathogenicity of the Variants

Conservation of the involved codon and domain across paralogous proteins from zebrafish to humans, a potential indicator of the biological significance of the codon, is shown in Figure 2. Likewise, the predicted effects of the nonsynonymous variants on MURC protein are shown in Table 4. Codon N128K affected a totally conserved amino acid from zebrafish to human and had a very high PolyPhen-2 prediction score (0.980; sensitivity, 0.69; specificity, 0.94), placing it in the probably damaging category (highest category).[13] The L153P also affected a highly conserved amino acid from rat *(Rattus norvegicus)* to human and was categorized as probably damaging (score, 0.975; sensitivity, 0.70; specificity, 0.94). The p.R140W and p.S364L involved conserved amino acids and were predicted to be possibly damaging (score for p.R140W, 0.840; sensitivity, 0.80; specificity, 0.90 and score for p.S364L, 0.438; sensitivity, 0.438; specificity, 0.86). In contrast, p.S307T and p.P324L involved fewer or nonconserved amino acids and were predicted to be benign.

Functional Characterization of *MURC* Mutations

We have previously shown that MURC activates the RhoA/ROCK pathway and its downstream target, ANP.[8] Therefore, we transduced NRCM with recombinant viruses expressing either a WT or a mutant MURC protein and measured RhoA activity. Expression of the WT MURC increased RhoA activity by ≈80%, a finding that is in accord with the previous data.[8] In contrast, RhoA activity was significantly less in myocytes expressing the mutant MURC proteins as compared with the WT MURC group (Figure 3).

Likewise, expression of the WT MURC significantly increased mRNA levels of ANP (Nppa) and SkA (Acat1) by >5-fold and that of BNP (Nppb) by ≈2.6-fold (Figure 3). In contrast, mRNA levels of the Nppa, Nppb, and Acta1 in NRCM transduced with the mutant MURC recombinant viruses were attenuated significantly, as compared with WT MURC. The findings indicate that the mutations impart a loss-of-function effect on the activation of RhoA and expression of the hypertrophic markers by MURC.

To further characterize the phenotypic consequence of the MURC mutations in vitro and complement the data on RhoA activity and expression of the molecular markers of hypertrophy, we measured the effects of expression of WT and mutant MURC proteins on cardiac myocyte size. Expression of the WT MURC increased cardiac myocyte surface area by ≈3.5-fold. However, the mutant MURC had attenuated hypertrophic effects, as myocyte surface area was significantly less in the mutant groups as compared with the WT MURC group (Figure 4).

Discussion

We have identified 6 DCM-specific heterozygous missense variants, including 4 that were predicted to be probably or possibly pathogenic. The mutations were associated with progressive heart failure, conduction defects, and cardiac arrhythmias. In vitro functional studies indicate loss-of-function effects of the mutant MURC proteins on activation of RhoA, expression of hypertrophic markers, and myocyte hypertrophy. Collectively, human molecular genetic and in vitro functional data implicate *MURC* as a causal gene for human DCM.

Several lines of evidence support the causal role of *MURC* mutations in DCM. All 6 nonsynonymous variants were

Table 3. Demographic, Echocardiographic, and ECG Phenotypes in DCM Patients With *MURC* Mutations

	AA Change	Ethnicity	Age at Diagnosis, y	Sex	BMI, kg/m^2	Clinical Phenotype	ST, cm	PWT, cm	LVEDD, cm	LVEF, %	ECG
1*	N128K	A	54	F	31.0	Heart failure, recurrent nonsustained V. Tach, ICD implantation, heart transplant	0.9	0.8	6.8	<10	SR, 1st-degree AV block, LAE, LVH with ST/T changes
2*		A	41	F	26.8	Heart failure, hypotension, nonsustained VT, SVT	0.8	0.9	6.3	28	SR, LVH with ST/T changes
3	R140W	C	41	M	25.9	SCA, ICD implantation, recurrent V. Fib, heart transplantation	1.2	1	6.6	26.5	A. Fib, atrial paced rhythm, LAE, LBBB, ST/T changes
4	L153P	A	48	M	23.0	Heart failure, NYHA functional class, cardiac thrombus	0.5	0.5	9.1	<10	SR, 1st-degree AV block, LAE, IVCD, V. Tach
5*	S307T	C	48	M	34	Heart failure, syncope, PPI, heart transplantation	0.8	0.9	6.9	<10	Ventricular paced rhythm
6*		C	36	M	47.3	Heart failure, palpitations, class III NYHA functional class on therapy	1.2	1.3	6.7	32	SR, IVCD
7*		C	33	F	24.8	Heart failure, syncope and V. Tach, ICD implantation, heart transplantation	1.3	1.3	7.4	<20	SR, LAE, LBBB
8	P324L (*TPM1:* M245T)	A	52	F	25.9	Heart failure, hypotension and low cardiac output requiring inotropic support, and LV assist device. Embolic stroke, PPI, and ICD	1.3 (0.9)	1.4 (1)	5 (5.5)	22	Dual-chamber paced rhythm, intermittent atypical AF, LVH with ST/T changes
9	P324L	A	49	F	47.2	Heart failure, class II NYHA functional class on medical therapy	0.8	1	5.4	32	SR, LVH voltage
10	P324L	A	46	M	27.4	Heart failure and palpitations, class IV NYHA functional class, evaluation for heart transplantation	0.8	1	5.4	32	SB, LVH with ST/T changes
11	S364L	A	47	M	49.7	Heart failure, palpitations, biventricular pacing (cardiac resynchronization therapy), ventricular support system, ICD	0.8	1	6.4	22	SR, LVH with ST/T, V. Tach

DCM indicates dilated cardiomyopathy; AA, amino acid; BMI, body mass index; ST, septal thickness; PWT, posterior wall thickness; LVEDD, left ventricular end-diastolic diameter; LVEF, left ventricular ejection fraction; SCA, sudden cardiac arrest; SR, sinus rhythm; LAE, left atrial enlargement; LVH, left ventricular hypertrophy; IVCD, intraventricular conduction delay; A. Fib, atrial fibrillation; LBBB, left bundle-branch block; V. Tach, ventricular tachycardia; V. Fib, ventricular fibrillation; SB, sinus bradycardia; AF, atrial flutter; NYHA, New York Heart Association; ICD, implantable cardioverter-defibrillator; and SVT, supraventricular tachycardia.

*Individuals 1 and 2 and individuals 5, 6, and 7 are family members. Echocardiographic data are findings on presentation. Data in parenthesis indicate findings on a follow-up echocardiogram. Individual 8 had increased left ventricular wall thickness with decreased LVEF at the time of first evaluation. She had subsequent development of a DCM phenotype.

absent in >500 control individuals who had no clinical, ECG, or echocardiographic evidence of cardiomyopathies. The variants were also absent in the dbSNP (build 132). A gene-centric analysis showed that the missense variants were overrepresented in patients with DCM by 25-fold. Likewise, 2 mutations cosegregated with the phenotype, albeit in small families. Although the de novo recurring mutations in cases only imply a causal role in DCM, the p.P324L recurring

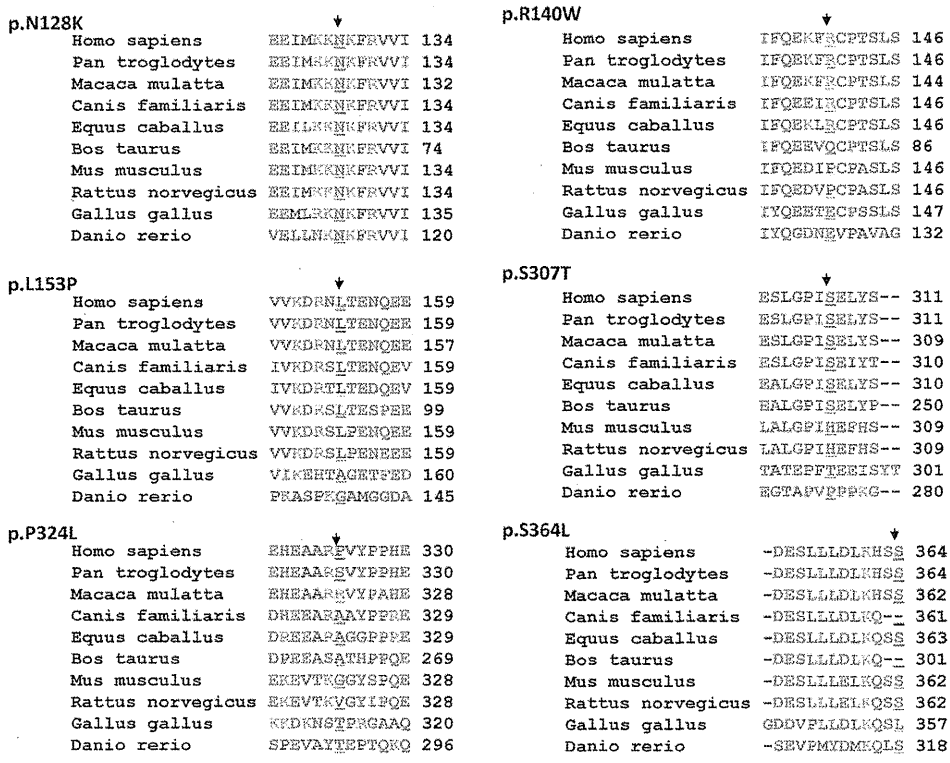

Figure 2. Multiple sequence alignment (MSA) of Muscle-Restricted Coiled-Coil (MURC) variants across species: MSA is performed using software package PRRN ((http://align.genome.jp/prrn/) to infer evolutionary conservation of the amino acids affected by the MURC nonsynonymous variants identified in probands with dilated cardiomyopathy. All available sequences from different species are included.

variant affected a nonconserved amino acid and was predicted to be benign by PolyPhen-2 analysis. Functional data, assessed at multiple levels, showed concordant results and indicated loss-of-function effects of the *MURC* mutations. Furthermore, 4 variants either involved largely conserved paralogous codons and/or were predicted to affect structure and biological function of the encoded protein. The findings are also in accord with the in vitro and in vivo biological functions of MURC protein and its potential involvement in myopathic conditions.[8–10]

MURC is a biologically plausible candidate gene for cardiomyopathies. MURC is a Z-line component protein that is predominantly expressed in the heart.[8–10] Mutations in genes encoding sarcomere and cytoskeletal proteins are major causes of cardiomyopathies.[4,5] MURC is involved in muscle protein homeostasis through regulating RhoA/ROCK and association with a multiprotein complex at the caveolae.[8–10] MURC interacts with extracellular signal-related kinases, RhoA/ROCK, and serum response factor pathways, which are also implicated in heart failure.[8,9,17] RhoA appears to play a delicate role in regulating cardiac function because its overexpression or its inhibition results in conduction defects and cardiac dysfunction.[18,19] Likewise, cardiac-restricted overexpression of MURC in mice leads to heart failure, conduction defect, and atrial arrhythmias.[8] Moreover, MURC is a component of a multiprotein complex in the caveolae that regulates cardiac function.[10] Its subcellular distribution is perturbed in human muscle disease associated with Caveolin-3 dysfunction.[10] Notably mutations in *CAV3*, encoding caveolin 3, are also known to cause cardiac and skeletal myopathy.[20,21]

The causal role of the *MURC* deletion mutation in HCM is less clear. Evidence in support of a potential causal role includes recurrence in 2 different ethnic populations and hence, occurring independently, its absence in >500 normal individuals and the increasing recognition of prevalence of

Table 4. Evolutionary Conservation and Biophysical Effects of the Putative Causal Variants

Amino Acid Change	Evolutionary Conservation	Charge Change	Change in Hydropathy	PolyPhen-2 Prediction
p.N128K	Conserved in all known proteins	Neutral to positive	−3.5 to −3.9	Probably damaging
p.R140W	Partially conserved	Positive to Neutral	−4.5 to −0.9	Possibly damaging
p.L153P	Highly conserved	Neutral	3.8 to −1.6	Probably damaging
p.S307T	Partially conserved	Neutral	−0.8 to −0.7	Benign
p.P324L	Nonconserved	Neutral	−1.6 to 3.8	Benign
p.S364L	Highly conserved	Neutral	−0.8 to 3.8	Possibly damaging

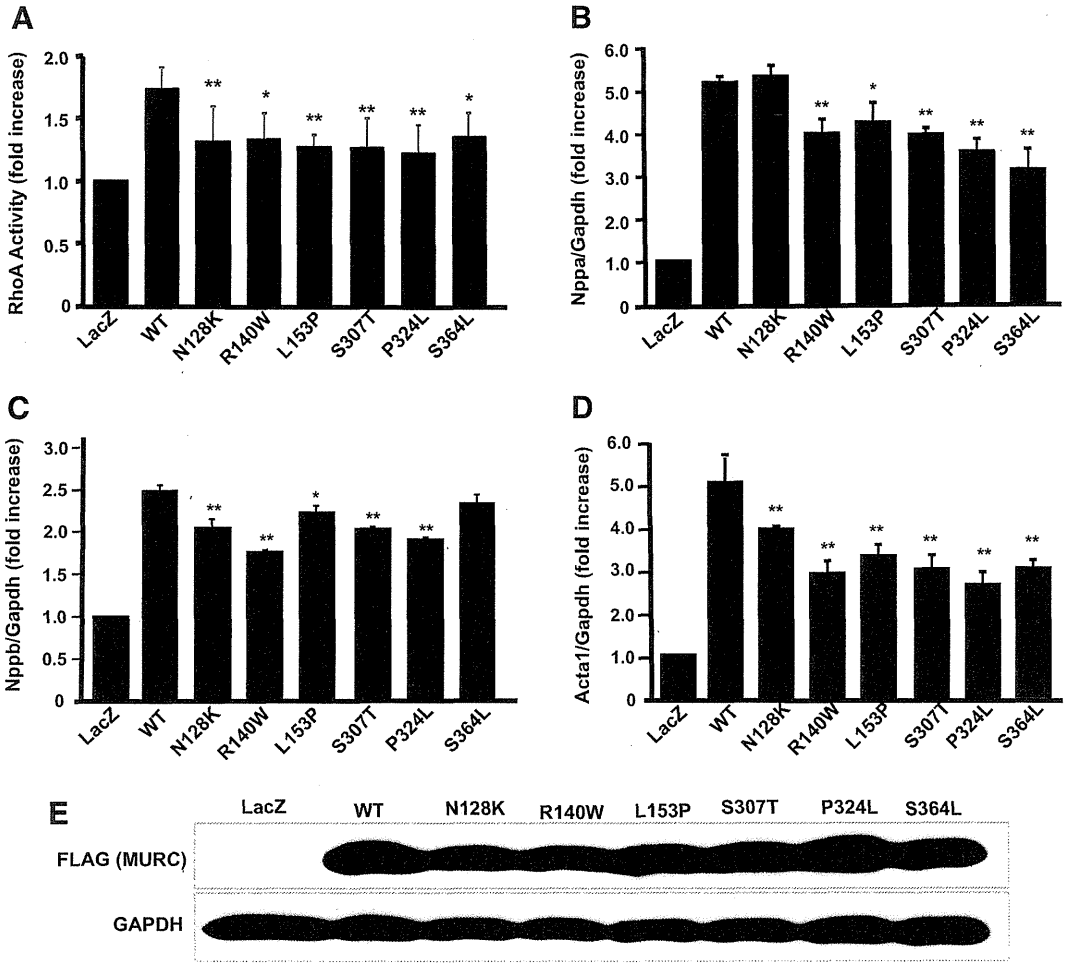

Figure 3. Effects of Muscle-Restricted Coiled-Coil (MURC) mutations on RhoA activation and expression of molecular markers of cardiac hypertrophy. **A**, Bar graph representing RhoA activity in neonatal rat cardiac myocytes (NRCM) infected with recombinant adenoviruses at a multiplicity of infection (MOI) of 10. The groups included Ad-LacZ (expressing β-galactosidase, as a control), wild-type human MURC (Ad-hMURC-WT), and each of the specific mutant MURCs (Ad-N128K, Ad-R140W, Ad-L153P, Ad-S307T, Ad-P324L, or Ad-S364L) that were identified in patients with dilated cardiomyopathy (DCM) (n=3 independent experiments per group. **B**, **C**, and **D**, MicroRNA expression levels of atrial natriuretic peptide (ANP; gene, *Nppa*), B-type or brain natriuretic peptide (BNP; gene name, *Nppb*), and skeletal α-actin (SkA; gene name, *Acta1*) in cardiac myocytes transduced at an MOI of 10 with control recombinant adenoviruses or viruses expressing WT or each of the 6 mutant MURC proteins. Cells were harvested 48 hours after the infection for extraction of RNA and quantitative reverse transcriptase–polymerase chain reaction. **E**, Immunoblot of myocytes proteins extracted 48 hours after transduction with the recombinant viruses and probed with an anti-FLAG antibody to detect expression of the WT or mutant MURC proteins (**upper blot**). Immunoblotting was performed to assess equal expression level of the WT and mutant MURC proteins among the groups. The **lower blot** shows expression of GAPDH, which was used as a control for loading conditions. *$P<0.05$ and **$P<0.01$ as compared with WT MURC.

compound mutations in cardiomyopathies.[22–25] However, the deletion variant was not present in an affected family member with the phenotype and hence, conventionally cannot be considered a causal variant in this family. The 2 affected members in this small family also had a missense mutation (p.L907V) in *MYH7*, which is predicted to be probably damaging. It is possible that the deletion variant codependently contributes to phenotypic expression of HCM in this family. These findings highlight the challenge of establishing the causal role of the DNA sequence variants in sporadic cases and small families, as opposed to large families, wherein cosegregation of the phenotype with inheritance of the variants (genetic linkage) could support the causality. While the actual LOD score is determined by the family structure and information content of the locus markers, typically >7 affected family members are necessary to achieve a significant LOD score in a linkage analysis of a familial disease with an autosomal dominant mode of inheritance, assuming 100% penetrance. Unfortunately, neither the number of the affected individuals in our families is adequate nor the penetrance is complete to perform a meaningful linkage analysis. The challenge is expected to have considerable clinical implications, as whole-exome or whole-genome sequencing gains clinical applications. The task is daunting because each diploid human genome contains >10 000 nonsynonymous variants, the majority of which are not associated with any discernible clinically phenotype (discussed in Reference 26).[26] Accordingly, several lines of genetic and functional data must be incorporated in discerning clinical significance of the DNA sequence variants in

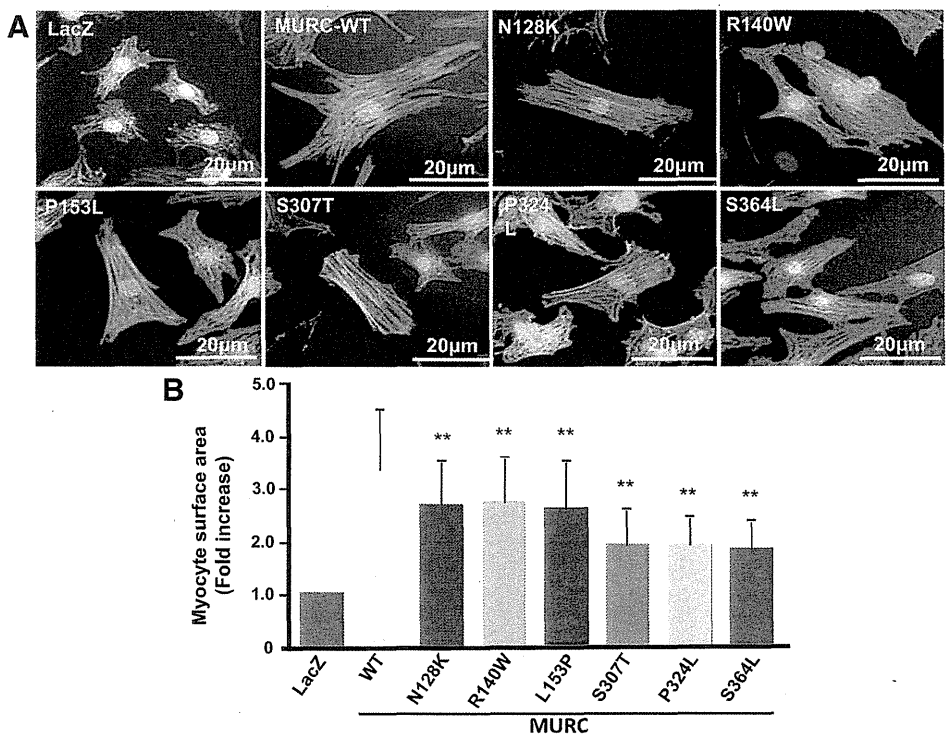

Figure 4. Induction of cardiac myocyte hypertrophy. **A**, Representative immunofluorescence images of neonatal rat cardiac myocytes (NRCM) transduced with a control virus or recombinant viruses, at a multiplicity of infection of 10, expressing wild-type (WT) mutant Muscle-Restricted Coiled-Coil (MURC) (Ad-LacZ, Ad-hMURC-WT, Ad-N128K, Ad-R140W, Ad-L153P, Ad-S307T, Ad-P324L, or Ad-S364L). Yellow bar indicates 20 μm scale. **B**, Bar graph depicting the mean and standard error of myocyte surface area in each experimental group. NRCM were infected with the recombinant viruses and stained with fluorescein isothiocyanate–conjugated phalloidin 48 hours after the transduction. Myocyte surface area was measured in at least 100 cells per group. $^{*}P<0.05$ and $^{**}P<0.01$ as compared with WT MURC.

sporadic cases or small families. Although our data strongly support the causal role of the MURC variants in DCM, one must consider the possibility that the *MURC* variants may not be true disease-causing variants but are susceptibility alleles that require a second mutation or injury to cause the clinical phenotype. There is also a possibility that these variants are functional variants that do not play significant roles in susceptibility to cardiomyopathies. We submit that the strengths of the genetic and functional data favor the causal role of *MURC* variants in the pathogenesis of human cardiomyopathies.

Acknowledgments

We thank T. Taniguchi, D. Naito, N. Nakanishi, and K. Miyagawa for technical assistance.

Sources of Funding

This study was supported by the National Heart, Lung, and Blood Institute (R01-088498); the National Institute of Aging (NIA) (R21 AG038597-01); a Burroughs Wellcome Award in Translational Research (No. 1005907); and the TexGen Fund from Greater Houston Community Foundation. Additional support was provided by the Ministry of Education, Culture, Sports, Science, and Technology of Japan (Drs Ueyama, Ogata, and Matsubara); Takeda Science Foundation (Dr Ogata); Mitsubishi Pharma Research Foundation (Dr Ueyama); and Japan Heart Foundation/Novartis Grant for Research Award on Molecular and Cellular Cardiology (Dr Ogata).

Disclosures

None.

References

1. Roger VL, Go AS, Lloyd-Jones DM, Adams RJ, Berry JD, Brown TM, Carnethon MR, Dai S, de Simone G, Ford ES, Fox CS, Fullerton HJ, Gillespie C, Greenlund KJ, Hailpern SM, Heit JA, Ho PM, Howard VJ, Kissela BM, Kittner SJ, Lackland DT, Lichtman JH, Lisabeth LD, Makuc DM, Marcus GM, Marelli A, Matchar DB, McDermott MM, Meigs JB, Moy CS, Mozaffarian D, Mussolino ME, Nichol G, Paynter NP, Rosamond WD, Sorlie PD, Stafford RS, Turan TN, Turner MB, Wong ND, Wylie-Rosett J. Heart disease and stroke statistics: 2011 update: a report from the American Heart Association. *Circulation.* 2011;123:459–463.
2. Wang L, Seidman JG, Seidman CE. Harnessing molecular genetics for the diagnosis and management of hypertrophic cardiomyopathy. *Ann Intern Med.* 2010;152:513–520.
3. Fatkin D, Graham RM. Molecular mechanisms of inherited cardiomyopathies. *Physiol Rev.* 2002;82:945–980.
4. Dellefave L, McNally EM. The genetics of dilated cardiomyopathy. *Curr Opin Cardiol.* 2010;25:198–204.
5. Marian AJ. Hypertrophic cardiomyopathy: from genetics to treatment. *Eur J Clin Invest.* 2010;40:360–369.
6. Knoll R, Hoshijima M, Hoffman HM, Person V, Lorenzen-Schmidt I, Bang ML, Hayashi T, Shiga N, Yasukawa H, Schaper W, McKenna W, Yokoyama M, Schork NJ, Omens JH, McCulloch AD, Kimura A, Gregorio CC, Poller W, Schaper J, Schultheiss HP, Chien KR. The cardiac mechanical stretch sensor machinery involves a z disc complex that is defective in a subset of human dilated cardiomyopathy. *Cell.* 2002;111:943–955.
7. Osio A, Tan L, Chen SN, Lombardi R, Nagueh SF, Shete S, Roberts R, Willerson JT, Marian AJ. Myozenin 2 is a novel gene for human hypertrophic cardiomyopathy. *Circ Res.* 2007;100:766–768.
8. Ogata T, Ueyama T, Isodono K, Tagawa M, Takehara N, Kawashima T, Harada K, Takahashi T, Shioi T, Matsubara H, Oh H. MURC, a muscle-restricted coiled-coil protein that modulates the Rho/ROCK pathway,

induces cardiac dysfunction and conduction disturbance. *Mol Cell Biol.* 2008;28:3424–3436.
9. Tagawa M, Ueyama T, Ogata T, Takehara N, Nakajima N, Isodono K, Asada S, Takahashi T, Matsubara H, Oh H. MURC, a muscle-restricted coiled-coil protein, is involved in the regulation of skeletal myogenesis. *Am J Physiol Cell Physiol.* 2008;295:C490–C498.
10. Bastiani M, Liu L, Hill MM, Jedrychowski MP, Nixon SJ, Lo HP, Abankwa D, Luetterforst R, Fernandez-Rojo M, Breen MR, Gygi SP, Vinten J, Walser PJ, North KN, Hancock JF, Pilch PF, Parton RG. MURC/cavin-4 and cavin family members form tissue-specific caveolar complexes. *J Cell Biol.* 2009;185:1259–1273.
11. Maron BJ, Towbin JA, Thiene G, Antzelevitch C, Corrado D, Arnett D, Moss AJ, Seidman CE, Young JB. Contemporary definitions and classification of the cardiomyopathies: an American Heart Association Scientific Statement from the Council on Clinical Cardiology, Heart Failure and Transplantation Committee; Quality of Care and Outcomes Research and Functional Genomics and Translational Biology Interdisciplinary Working Groups; and Council on Epidemiology and Prevention. *Circulation.* 2006;113:1807–1816.
12. Cresci S, Kelly RJ, Cappola TP, Diwan A, Dries D, Kardia SL, Dorn GW II. Clinical and genetic modifiers of long-term survival in heart failure. *J Am Coll Cardiol.* 2009;54:432–444.
13. Sunyaev S, Ramensky V, Koch I, Lathe W III, Kondrashov AS, Bork P. Prediction of deleterious human alleles. *Hum Mol Genet.* 2001;10:591–597.
14. Alcalai R, Seidman JG, Seidman CE. Genetic basis of hypertrophic cardiomyopathy: from bench to the clinics. *J Cardiovasc Electrophysiol.* 2008;19:104–110.
15. Ashrafian H, Watkins H. Reviews of translational medicine and genomics in cardiovascular disease: new disease taxonomy and therapeutic implications cardiomyopathies: therapeutics based on molecular phenotype. *J Am Coll Cardiol.* 2007;49:1251–1264.
16. Lombardi R, Dong J, Rodriguez G, Bell A, Leung TK, Schwartz RJ, Willerson JT, Brugada R, Marian AJ. Genetic fate mapping identifies second heart field progenitor cells as a source of adipocytes in arrhythmogenic right ventricular cardiomyopathy. *Circ Res.* 2009;104:1076–1084.
17. Chang J, Wei L, Otani T, Youker KA, Entman ML, Schwartz RJ. Inhibitory cardiac transcription factor, srf-n, is generated by caspase 3 cleavage in human heart failure and attenuated by ventricular unloading. *Circulation.* 2003;108:407–413.
18. Sah VP, Minamisawa S, Tam SP, Wu TH, Dorn GW, Ross J, Chien KR, Brown JH. Cardiac-specific overexpression of RhoA results in sinus and atrioventricular nodal dysfunction and contractile failure. *J Clin Invest.* 1999;103:1627–1634.
19. Wei L, Taffet GE, Khoury DS, Bo J, Li Y, Yatani A, Delaughter MC, Klevitsky R, Hewett TE, Robbins J, Michael LH, Schneider MD, Entman ML, Schwartz RJ. Disruption of rho signaling results in progressive atrioventricular conduction defects while ventricular function remains preserved. *FASEB J.* 2004;18:857–859.
20. Minetti C, Sotgia F, Bruno C, Scartezzini P, Broda P, Bado M, Masetti E, Mazzocco M, Egeo A, Donati MA, Volonte D, Galbiati F, Cordone G, Bricarelli FD, Lisanti MP, Zara F. Mutations in the caveolin-3 gene cause autosomal dominant limb-girdle muscular dystrophy. *Nat Genet.* 1998;18:365–368.
21. Hayashi T, Arimura T, Ueda K, Shibata H, Hohda S, Takahashi M, Hori H, Koga Y, Oka N, Imaizumi T. Identification and functional analysis of a caveolin-3 mutation associated with familial hypertrophic cardiomyopathy. *Biochem Biophys Res Commun.* 2004;313:178–184.
22. Blair E, Price SJ, Baty CJ, Ostman-Smith I, Watkins H. Mutations in cis can confound genotype-phenotype correlations in hypertrophic cardiomyopathy. *J Med Genet.* 2001;38:385–388.
23. Van Driest SL, Vasile VC, Ommen SR, Will ML, Tajik AJ, Gersh BJ, Ackerman MJ. Myosin binding protein c mutations and compound heterozygosity in hypertrophic cardiomyopathy. *J Am Coll Cardiol.* 2004;44:1903–1910.
24. Bezzina CR, Rook MB, Groenewegen WA, Herfst LJ, van der Wal AC, Lam J, Jongsma HJ, Wilde AA, Mannens MM. Compound heterozygosity for mutations (w156x and r225w) in scn5a associated with severe cardiac conduction disturbances and degenerative changes in the conduction system. *Circ Res.* 2003;92:159–168.
25. Jeschke B, Uhl K, Weist B, Schroder D, Meitinger T, Dohlemann C, Vosberg HP. A high risk phenotype of hypertrophic cardiomyopathy associated with a compound genotype of two mutated beta-myosin heavy chain genes. *Hum Genet.* 1998;102:299–304.
26. Marian AJ. Nature's genetic gradients and the clinical phenotype. *Circ Cardiovasc Genet.* 2009;2:537–539.

CLINICAL PERSPECTIVE

Heart failure is a major cause of mortality and morbidity. Genetic mutations are important causes of susceptibility to heart failure. Familial dilated cardiomyopathy (DCM) is a classic form of systolic heart failure caused by genetic mutations. The known causal genes for DCM typically code for sarcomere and cytoskeletal proteins. Prompted by the experimental data, which implicate Muscle-Restricted Coiled-Coil (MURC) in regulating cardiac function, we investigated the causal role of the *MURC* gene in DCM. We sequenced the protein coding regions of *MURC* in 383 probands with DCM, 307 with hypertrophic cardiomyopathy, and 509 healthy control subjects. We found 6 missense mutations that were present only in DCM patients and were absent in control subjects. Two of these mutations segregated with inheritance of DCM in small families. One mutation recurred in 3 independent probands, including 1 proband who also had another mutation in the α-tropomyosin gene. We also found 1 deletion mutation in 3 unrelated probands with hypertrophic cardiomyopathy that might be a causative or susceptibility variant. The clinical features associated with *MURC* mutations included progressive heart failure that often led to heart transplantation, conduction defects, and atrial arrhythmias. Studies in cultured cardiac myocytes showed that the mutations reduced RhoA activity, an important signal transducer in the heart and impaired myocyte hypertrophic response. We conclude that *MURC* probably is a causal gene for DCM. We suggest elucidation of the molecular genetic and pathogenesis of heart failure is an essential step in the ultimate treatment of this potentially deadly disease.

SUPPLEMENTAL MATERIAL

CIRCCVG/2011/959866

Molecular Genetic and Functional Characterization Implicate Muscle-Restricted Coiled-Coil Gene (*MURC*) As a Causal Gene For Familial Dilated Cardiomyopathy

Gabriela Rodriguez, MD, et al.

TABLE 1

A. Sequence of Oligonucleotide Primers Used for Sequencing of *MURC* Exons

(Genomic DNA Sequence Source: NC_000009.11, GI:224589821)

Exon 1 (nucleotides 5- 586)

Forward: 5'CCTGTTGCCTGTTATCAAGCTGAC3'

Reverse: 5'GACACTGGAAACCTCTGATATGAC3'

Exon 2 - Fragment 1 (nucleotides 7637 - 8058)

Forward: 5'CATGGCCAGAAGGTAAAAGAGCTG3'

Reverse: 5'CCTGACTGTCTCAGCCTCTCTC3'

Exon 2 - Fragment 2 (nucleotides 7930 - 8475)

Forward: 5'GACACGGCAGAATCTTGACAAG3'

Reverse: 5'CATGGCACAGAAATGTAGACGAC3'

B. Sequence of Oligonucleotide Primers Used for Mutagenesis

p.N128K

Forward: 5'GTCAAGCAAGAGGAAATAATGAAGAAAAAGAAATTCCGCGTGG3'

Reverse: 5'-CCACGCGGAATTTCTTTTTCTTCATTATTTCCTCTTGCTTGAC3'

p.R140W

Forward: 5'-CAGGAGAAGTTTTGGTGTCCGACATCCCTGTCTG3'

Reverse: 5'-CAGACAGGGATGTCGGACACCAAAACTTCTCCTG3'

p.L153P

Forward: 5'-GTCTGTTGTTAAAGACAGAAACCCAACTGAGAACCAAGAAGAGG3'

Reverse: 5'-CCTCTTCTTGGTTCTCAGTTGGGTTTCTGTCTTTAACAACAGAC3'

p.S307T

Forward: 5'-GTCTCTGGGCCCCATCACTGAGCTCTACTCTG3'

Reverse: 5'-CAGAGTAGAGCTCAGTGATGGGGCCCAGAGAC3'

p.P324L

Forward: 5'-GAACACGAGGCAGCCAGGCTGGTGTATCCTCCCCATGAAG3'

Reverse: 5'-CTTCATGGGGAGGATACACCAGCCTGGCTGCCTCGTGTTC3'

p.S364L

Forward: 5'-GATTTAAAGCACTCATTGGACTACAAAGACGATGACGAC3'

Reverse: 5'-GTCGTCATCGTCTTTGTAGTCCAATGAGTGCTTTAAATC3'

C. Sequence of Oligonucleotide Primers Used in qPCR

Rat atrial natriuretic peptide (ANP or *Nppa*)

Forward: 5'-ATACAGTGCGGTGTCCAACA-3'

Reverse: 5'-CGAGAGCACCTCCATCTCTC-3'

Rat brain natriuretic peptide (BNP or *Nppb*)

Forward: 5'-GGAAATGGCTCAGAGACAGC-3'

Reverse: 5'-CGATCCGGTCTATCTTCTGC-3'

Rat skeletal α-actin (SkA or *Acta1*)

Forward: 5'-CACGGCATTATCACCAACTG-3'

Reverse: 5'-CCGGAGGCATAGAGAGACAG-3'

Rat glyceraldehyde-3-phosphate dehydrogenase (*Gapdh*)

Forward: 5'-ATGGGAAGCTGGTCATCAAC-3'

Reverse: 5'-GTGGTTCACACCCATCACAA-3'

Online Supplementary Material

TABLE 2

Non-Synonymous Variants Identified in the Probands and Controls

Variants		Controls		DCM		HCM	
		N=509		N=383		N=307	
		AA	C	AA	C	AA	C
		316	193	179	204	49	258
AA	Nucleotide						
p.S20T	g. 149G>C	2	0	1	0	0	0
p.S78L	g.323C>T	13	0	6	1	2	0
p.N81K	g.333T>G	1	0	1	0	1	0
p.R131H	g.482G>A	1	2	2	1	0	0
p.D163G	g.7791A>G	9	0	4	0	1	0
p.R231K	g.7795G>A	2	0	0	0	1	0
Total number of non-synonymous variants per group and ethnic background		28	2	14	2	5	0
Total number of non-synonymous variants per group		30 (5.9%)		16 (4.2%)		5 (1.6%)	

The prevalence of these non-synonymous variants was not significantly different between the DCM probands and controls. Likewise, the mean and median ages of individuals with these rare non-synonymous variants in the control and the DCM groups were similar (mean: 48.7 ± 8.6 vs. 47.9 ± 3.9, respectively, p=0.537; median: 45 vs. 49 years; range: 22 to 81 vs. 23 to 72 years).

Online Supplementary Material

Table 3

Synonymous, non-coding and deletion variants identified in the study population

Study Population		Total	Control		DCM		HCM	
			AA	C	AA	C	AA	C
		1,199	316	193	179	204	49	258
Nucleotide	Amino acid	Number of Individuals with DNA Sequence variants						
		1,183	264	233	178	211	47	250
g.34G>A	Non-coding	10	1	3	3	2	1	0
g.34G>R	Non-coding	6	1	0	0	5	0	0
g.79G>R	Non-coding	1	0	0	1	0	0	0
g.147G>R	p.S19S	5	2	0	2	0	1	0
g.267G>R	p.R59R	1	0	1	0	0	0	0
g.339G>K	p.G83G	1	0	0	0	1	0	0
g.504C>M	Non-coding	11	4	0	7	0	0	0
g.507G>R	Non-coding	2	0	0	1	0	1	0
g.526T>Y	Non-coding	3	1	0	2	0	0	0
g.540T>C	Non-coding	75	10	21	7	13	2	22
g.540T>Y	Non-coding	361	96	75	43	63	10	74
g.7729G>R	p.P142P	1	0	0	0	0	1	0
g.7822G>S	p.S173S	1	0	0	0	0	0	1
g.7873A>T	p.S190S	1	0	0	1	0	0	0
g.7873A>W	p.S190S	81	26	8	25	5	6	11
g.7918A>R	p.E205E	3	2	0	1	0	0	0
g.7981G>K	p.V226V	1	0	0	1	0	0	0
g.7987G>R	p.P228P	1	0	0	1	0	0	0
g. 8005A>R	p.L234L	5	0	1	0	1	0	3
g. 8008G>R	p.R235R	6	0	2	0	1	0	3
g.8017A>R	p.G238G	1	0	1	0	0	0	0
g.8203C>Y	p.S300S	1	1	0	0	0	0	0
g.8299G>A	p.R332R	150	17	33	15	29	6	50
g.8299G>R	p.R332R	434	94	87	60	89	18	86
g.8427A>R	Non-coding	3	0	1	0	2	0	0
g.8444T>Y	Non-coding	18	9	0	8	0	1	0

Online Figure 1

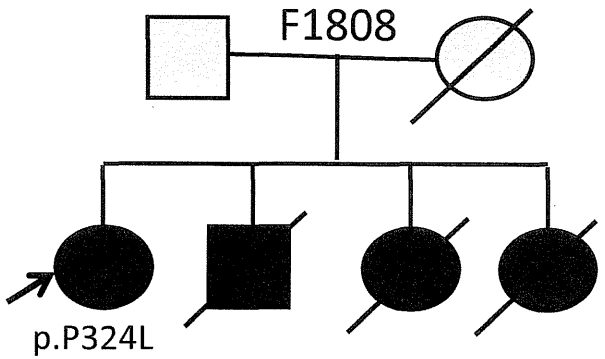

D9S180	231/233
D9S910	110/125
D9S176	151/153

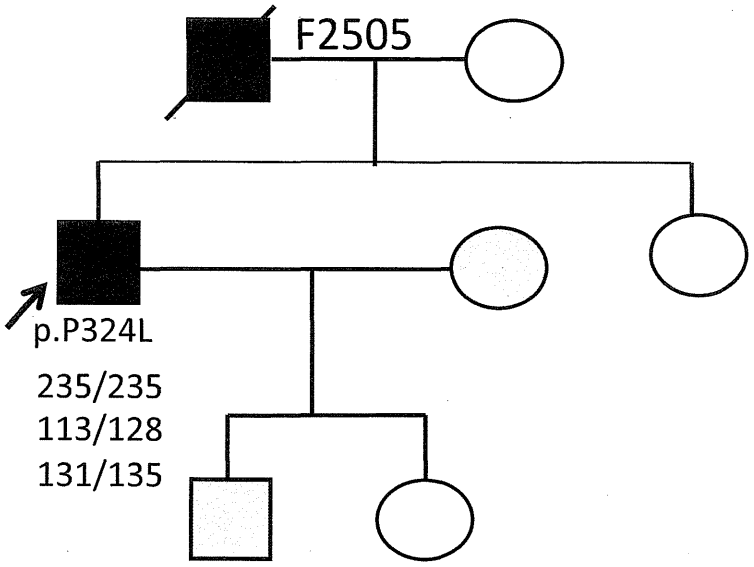

D9S180	235/235
D9S910	113/128
D9S176	131/135

D9S180	235/235
D9S910	110/113
D9S176	131/143

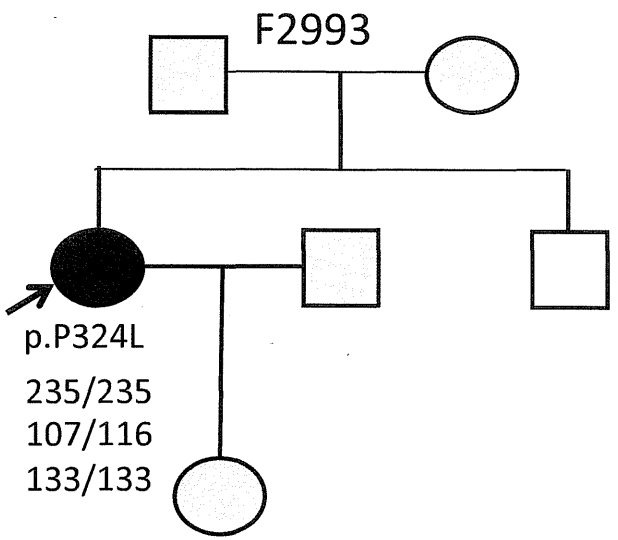

D9S180	235/235
D9S910	107/116
D9S176	133/133

Online Figure 2

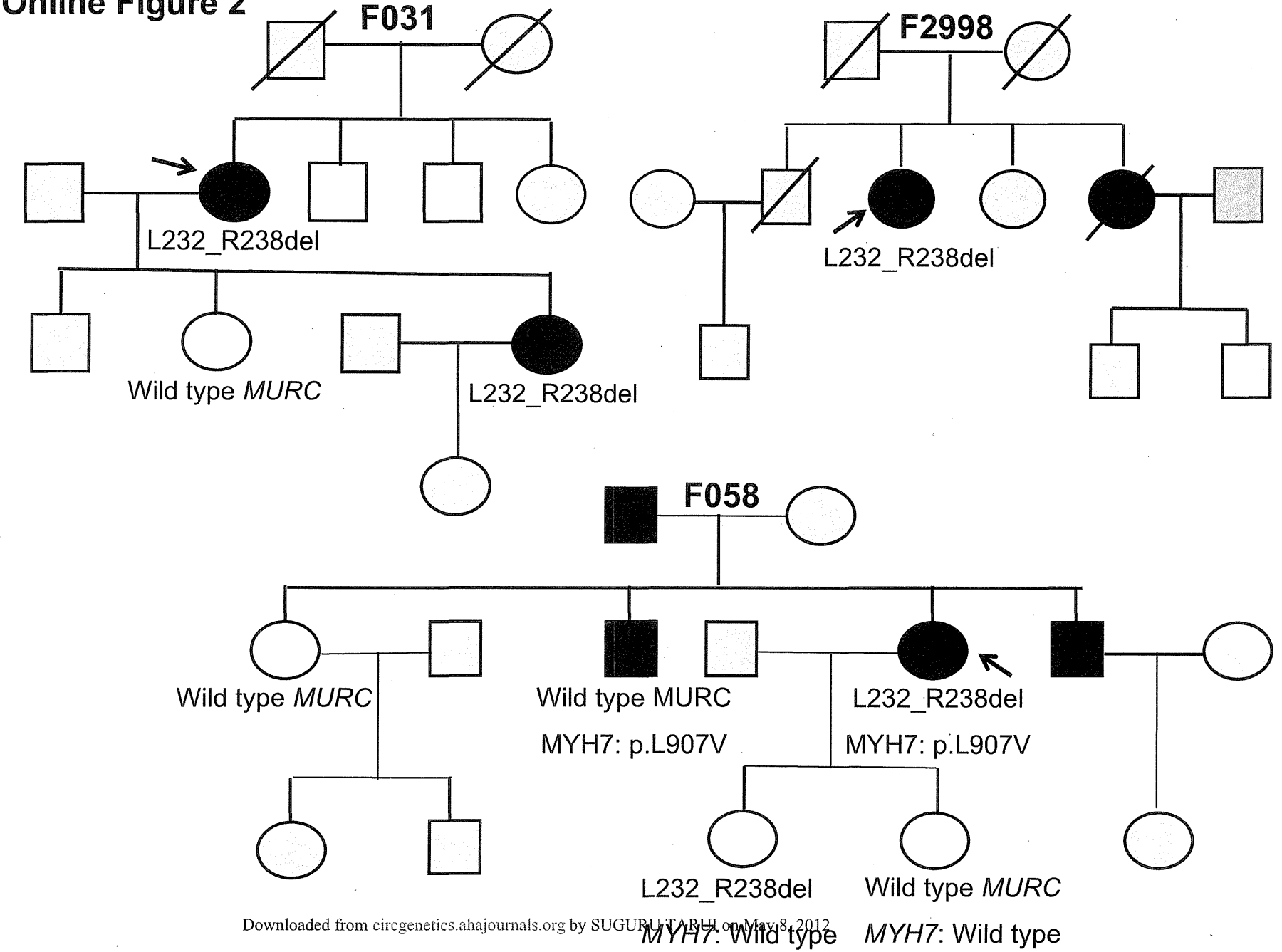

Supplemental figure legend

Supplemental Figure 1. Genotypes of three probands with familial dilated cardiomyopathy and the p.P324L variant in *MURC* gene, who were typed for three short tandem repeat markers at the *MURC* locus. As shown the probands do not share a common locus haplotypes, indicating an independent origin of the p.P324L variants in three probands. Pedigree symbols are per convention (full circles and squares indicate affected females and males respectively. Empty circles and squares indicate normal females and males respectively. Grey symbols indicate individuals that were not phenotyped.

Supplemental Figure 2. Detection of the deletion variant (L232-R238del) in three families with hypertrophic cardiomyopathy. The deletion variant did not co-segregate with the phenotype in Family F058 as one clinically affected family member did not have the deletion mutation. A second mutation p.L907V in MYH7 was detected in two affected members in this family. Symbols are as in Supplemental Figure 1.

PARM-1 Is an Endoplasmic Reticulum Molecule Involved in Endoplasmic Reticulum Stress-Induced Apoptosis in Rat Cardiac Myocytes

Koji Isodono[1,2], Tomosaburo Takahashi[1,2]*, Hiroko Imoto[1,2], Naohiko Nakanishi[1], Takehiro Ogata[1,2], Satoshi Asada[1,2], Atsuo Adachi[1,2], Tomomi Ueyama[1,2], Hidemasa Oh[1,2], Hiroaki Matsubara[1,2]

1 Department of Cardiovascular Medicine, Kyoto Prefectural University of Medicine, Kyoto, Japan, **2** Department of Experimental Therapeutics, Translational Research Center, Kyoto University Hospital, Kyoto, Japan

Abstract

To identify novel transmembrane and secretory molecules expressed in cardiac myocytes, signal sequence trap screening was performed in rat neonatal cardiac myocytes. One of the molecules identified was a transmembrane protein, prostatic androgen repressed message-1 (PARM-1). While PARM-1 has been identified as a gene induced in prostate in response to castration, its function is largely unknown. Our expression analysis revealed that PARM-1 was specifically expressed in hearts and skeletal muscles, and in the heart, cardiac myocytes, but not non-myocytes expressed PARM-1. Immunofluorescent staining showed that PARM-1 was predominantly localized in endoplasmic reticulum (ER). In Dahl salt-sensitive rats, high-salt diet resulted in hypertension, cardiac hypertrophy and subsequent heart failure, and significantly stimulated PARM-1 expression in the hearts, with a concomitant increase in ER stress markers such as GRP78 and CHOP. In cultured cardiac myocytes, PARM-1 expression was stimulated by proinflammatory cytokines, but not by hypertrophic stimuli. A marked increase in PARM-1 expression was observed in response to ER stress inducers such as thapsigargin and tunicamycin, which also induced apoptotic cell death. Silencing PARM-1 expression by siRNAs enhanced apoptotic response in cardiac myocytes to ER stresses. PARM-1 silencing also repressed expression of PERK and ATF6, and augmented expression of CHOP without affecting IRE-1 expression and JNK and Caspase-12 activation. Thus, PARM-1 expression is induced by ER stress, which plays a protective role in cardiac myocytes through regulating PERK, ATF6 and CHOP expression. These results suggested that PARM-1 is a novel ER transmembrane molecule involved in cardiac remodeling in hypertensive heart disease.

Citation: Isodono K, Takahashi T, Imoto H, Nakanishi N, Ogata T, et al. (2010) PARM-1 Is an Endoplasmic Reticulum Molecule Involved in Endoplasmic Reticulum Stress-Induced Apoptosis in Rat Cardiac Myocytes. PLoS ONE 5(3): e9746. doi:10.1371/journal.pone.0009746

Editor: Arnold Schwartz, University of Cincinnati, United States of America

Received December 10, 2009; **Accepted** February 28, 2010; **Published** March 18, 2010

Funding: This work was supported by Grants-in-Aid from the Ministry of Education, Culture, Sports, Science and Technology of Japan, a grant from the Mitsubishi Pharma Research Foundation and Grants-in-Aid from the Ministry of Health, Labor and Welfare of Japan. The funders had no role in study design, data collection and analysis, decision to publish, or preparation of the manuscript.

Competing Interests: The authors have declared that no competing interests exist.

* E-mail: ttaka@koto.kpu-m.ac.jp

Introduction

Chronic heart failure is a major and increasing public health problem, especially in industrialized societies with aging populations. The rate of hospital admission has increased progressively over the past years, making heart failure one of the most common indications for hospital admission in elderly people [1]. Considerable therapeutic advances including pharmacotherapy such as blockade of renin-angiotensin system and β adrenergic receptor, and nonpharmacologic therapies such as heart transplantation and resynchronization therapy have been made in recent years. However, mortality among patients with heart failure remains still substantial, and the well-beings deteriorate dramatically, underscoring the need for additional therapeutic options [2]. Since there may be significant potential in therapies targeting the novel pathological pathways, it is crucial to understand the molecular mechanisms involved in cardiac pathophysiology, especially ones specifically operated in the hearts.

Apoptosis is a process of innate cellular death, controlled by complex and diverse molecular mechanisms with considerable cell type specificity. Apoptosis plays important roles in various aspects of biology from development to a wide range of diseases such as cancers and cardiovascular diseases. In the heart, apoptosis is essential for cardiac development such as formation of cardiac valves and outflow tract [3]. Although apoptosis is rare in normal human hearts, the rate of cardiac myocyte apoptosis can increase several hundred fold in dilated and ischemic cardiomyopathies, hypertensive heart disease and arrhythmogenic right ventricular dysplasia, and an association between apoptosis, cardiac myocyte loss, ventricular remodeling and deterioration of systolic performance has been demonstrated in multiple experimental models [4,5]. Although apoptotic processes are tightly regulated by extracellular factors and intracellular signalings, the precise molecular mechanisms governing cardiac myocyte apoptosis have not been fully elucidated, and understanding the regulation of apoptosis is of great importance for the advancement of cardiac biology and for developing novel therapeutic strategies.

In this study, we sought to identify a novel molecule involved in cardiac pathophysiology using efficient signal sequence trap method. Signal sequence trap is a strategy to specifically clone

cDNA fragments with signal sequence, a short hydrophobic stretch of amino acids which mediates targeting of secreted and cell-surface proteins to the cell membrane [6,7]. As secreted and membrane molecules play critical roles in cellular functions and interactions, and are potential therapeutic targets for antagonistic or agonistic strategies, this strategy could be useful to identify novel molecules involved in cardiac pathophysiology. Among the molecules identified, in this study, we analyzed the role of prostatic androgen repressed message-1 (PARM-1) [8] in cardiac myocytes.

Results

Identification of PARM-1 as an endoplasmic reticulum protein expressed in cardiac myocytes

In this study, we applied the efficient signal sequence trap cloning using retrovirus-mediated gene transfer to identify novel transmembrane and secreted molecules expressed in cardiac myocytes [6,9]. Among the molecules identified (Table 1), a transmembrane protein, PARM-1, was selected for further analysis, because its expression and functions in cardiac myocytes were largely unknown. Our expression analysis revealed that PARM-1 was most abundantly expressed in hearts (Fig. 1A). PARM-1 was also expressed in skeletal muscles and stomachs. These results suggested that PARM-1 could be expressed in striated and smooth muscles. To identify a cell type expressing PARM-1 in the hearts, we separated cardiac myocytes and non-myocytes from neonatal hearts, and expression of PARM-1 in cardiac myocytes and non-myocytes was analyzed. As shown in Fig. 1B, PARM-1 transcript was specifically expressed in cardiac myocytes, but not in non-myocytes, indicating that the major source of PARM-1 in the hearts is cardiac myocytes. To evaluate how PARM-1 expression is regulated during heart development, we analyzed mRNA expression in hearts of embryos, neonates and adult mice (Fig. 1C). PARM-1 mRNA expression in the heart was detected at embryonic day 10.5 (E10.5), increased until neonatal stages and, thereafter remained unchanged through adult stages. To assess subcellular localization of PARM-1 in cardiac myocytes, flag-tagged PARM-1 was expressed in cultured neonatal cardiac myocytes, and the cells were stained with anti-flag antibody.

Table 1. Signal sequence trap screening of cultured neonatal cardiac myocytes.

Symbol	protein name	clone number
Spark	secreted acidic cysteine rich glycoprotein	33
Nppa	natriuretic peptide precursor type A	13
Tmem9	transmembrane protein 9 (predicted)	10
Coll8a1	procollagen, type XVIII, alpha 1	10
Podxl	podocalyxin-like	8
Gpc1	glypican 1	6
Fxyd5	FXYD domain-containing ion transport regulator 5	5
Parm1	prostatic androgen repressed message 1	5
Col4a1	procollagen, type IV, alpha 2 (predicted)	4
Col1a1	procollagen, type 1, alpha 1	4
Srl	sarcalumenin	4
Sdc3	syndecan 3	4
Jun	Jun oncogene	3
Dlk1	delta-like 1 homolog (Drosophila)	3
Igfbp3	insulin-like growth factor binding protein 3	3
Col4a2	procollagen, type IV, alpha 1	2
Pi16	protease inhibitor 16 (predicted)	2
Notch3	Notch gene homolog 3	2
Tmem9 sf4	transmembrane 9 superfamily protein member 4	1
RGD1562476	similar to Eso3 protein (predicted)	1
Pecam	platelet/endothelial cell adhesion molecule	1
Gnai2	guanine nucleotide binding protein, alpha inhibiting 2	1
Sparcl1	SPARC-like 1	1
Atp6ap2	ATPase, H+ transporting, lysosomal accessory protein 2	1
Myadm	myeloid-associated differentiation marker	1
Apoe	apolipoprotein E	1
Fstl1	follistatin-like 1	1
Hspa5	heat shock 70 kDa protein 5 (glucose-regulated protein)	1
Sfrp1	secreted frizzled-related protein 1	1
Cd320	CD320 antigen	1
Canx	Calnexin	1

doi:10.1371/journal.pone.0009746.t001

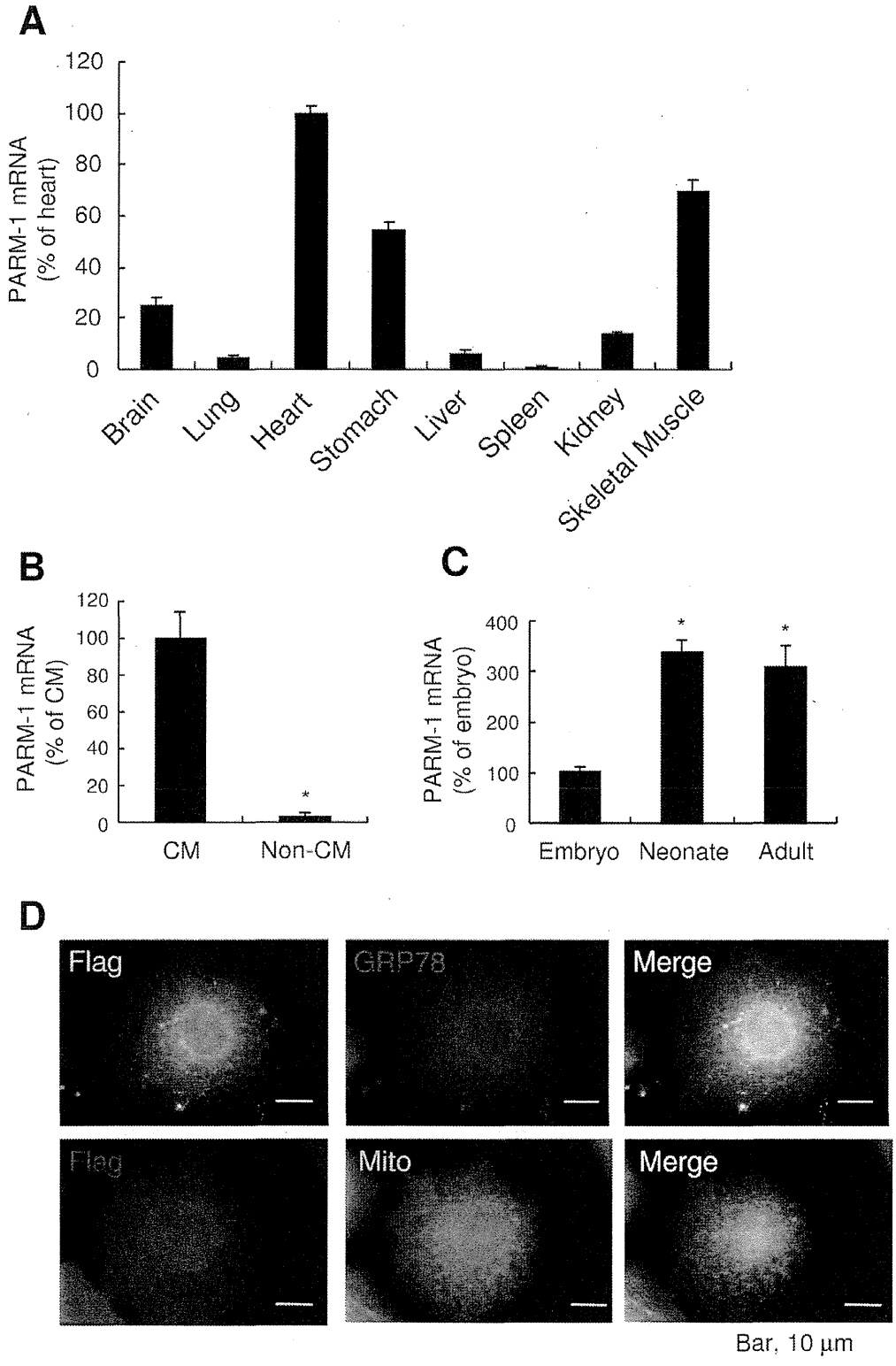

Figure 1. PARM-1 is an ER protein expressed in cardiac myocytes. *A, B, C*: PARM-1 expression was assessed by kinetic real-time RT-PCR in various tissues of adult mice (A), cultured rat neonatal cardiac myocytes and non-myocytes (B), and developmental mouse hearts (C), respectively. *$P<0.05$ versus cardiac myocytes (B) or embryonic hearts (C). *D*: Cellular localization of PARM-1 was analyzed by immunostaining of cultured neonatal rat cardiac myocytes expressing flag-tagged PARM-1 with anti-Flag antibody (left), and anti-GRP78 antibody or MitoTacker (center). Nuclei were stained by DAPI.
doi:10.1371/journal.pone.0009746.g001